A theoretical investigation of electron–lattice interaction on Fe warwickites

2006 J. Phys.: Condens. Matter 18 8267

(http://iopscience.iop.org/0953-8984/18/35/013)

INSTITUTE OF PHYSICS PUBLISHING JOURNAL OF PHYSICS: CONDENSED MATTER

J. Phys.: Condens. Matter **18** (2006) 8267–8280 doi:10.1088/0953-8984/18/35/013

A theoretical investigation of electron–lattice interaction on Fe warwickites

M Matos and R B Oliveira

Departamento de Física, PUC-Rio, Gávea, CEP 22453-970, Caixa Postal 38071, Rio de Janeiro, RJ, Brazil

Received 11 April 2006, in final form 19 July 2006
Published 18 August 2006
Online at stacks.iop.org/JPhysCM/18/8267

Abstract

A theoretical electronic structure study is performed on two crystalline phases of the mixed valence, charge ordering Fe_2OBO_3 warwickite and on a V substituted compound, $Fe_{1.91}V_{0.09}OBO_3$, known to exhibit no charge ordering or structural transitions. By using the extended Hückel method applied to the high spin band (hsb) filling scheme, calculations on bulk and on several crystal sub-units have shown that local monoclinic distortions lead to a decrease in Fe–Fe dimer interaction strength. It is suggested that changes in metal–metal interactions between two Fe sub-lattices stabilize local charge arrangements in the monoclinic phase, possibly set in through other effects such as electrostatic long range interactions, discussed in the literature. The importance of electron–lattice interactions in charge localization and structural transition of Fe_2OBO_3 is further corroborated by calculations in the substituted compound, which show that V acts so as to hinder inter-ribbon Fe–Fe interactions. It is also shown that the use of hsb gives very good results for the prediction of charge distribution in the pure and substituted warwickites.

1. Introduction

The homometallic oxy-borate Fe_2OBO_3, of the warwickite group, is an interesting example of mixed valence metal oxide [1]. The material undergoes at 317 K a structural transition from the orthorhombic to the monoclinic symmetry. The structural change occurs approximately midway through a broad semiconductor–semiconductor transition [2–4], which is also associated with charge localization. In Fe_2OBO_3, however, charge ordering is not clearly related to local geometrical distortions due to the structural transition. For example, below 270 K, Mössbauer spectroscopy data [2–4] have revealed that Fe^{2+} and Fe^{3+} ions are equally distributed over crystallographically distinct metal sites, indicating electronic equivalence of sites. It has been proposed [1] that, in this material, charge ordering takes advantage of electrostatic repulsion of the extra Fe^{2+} electrons which is stabilized in the monoclinic structure. This is essentially different from the localization process of another homometallic warwickite, Mn_2OBO_3, of very similar structure, wherein charge ordering is related to orbital

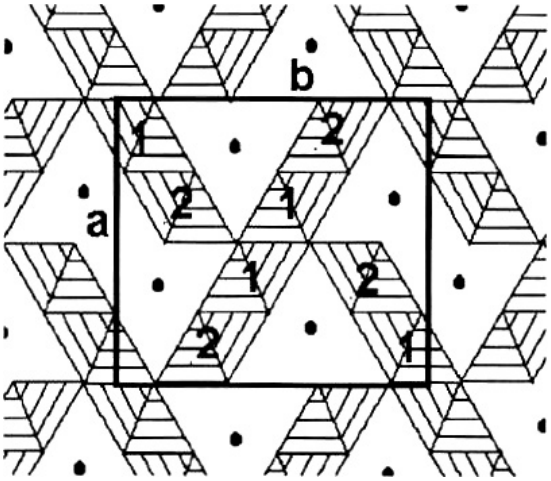

Figure 1. The polyhedral representation of the warwickite crystal structure projected in the *ab* plane. The *a* and *b* edges of the unit cell and the two distinct metal sites are indicated. The central 2–1–1–2 oxygen octahedron row constitutes the building block of one ribbon, which grows along *c*. The two halves of two other ribbons complete the unit cell. Boron atoms: black dots.

order which sets in by local distortions in Mn^{3+} sites [5, 6]. More recently, however, the role of electron–lattice interactions in the charge ordering state of Fe_2OBO_3 has been reviewed, in face of *ab initio* calculations on the monoclinic structure of this material [7].

Resistivity versus temperature curves have shown hopping activated behaviour with activation energies around 0.3 eV in both regimes, below and above the 317 K transition [1, 3]. On the other hand, magnetic order was observed only below 155 K, being characterized as a ferrimagnetic alignment of the different spins of Fe^{2+} ($S = 2$) and Fe^{3+} ($S = 5/2$) [2, 3, 8]. Attfield *et al* [1] point out that, in contrast to magnetite, where conductivity takes advantage of magnetic order, in Fe_2OBO_3 conductivity is hindered by the fact that the ferrimagnetic temperature (155 K) is much lower than that of charge ordering (317 K).

The warwickites are oxy-borates of chemical formula $M^{2+}M'^{3+}OBO_3$ with the metal ions found at the centre of oxygen octahedra which group themselves through common edges or corners [5, 9]. They form monoclinic or orthorhombic crystals with flat unit cells ($a, b \sim 9$ Å, $c \sim 3$ Å). By piling up a string of four octahedra along the short crystallographic axis, 1D structures (ribbons) are formed which are interconnected by the boron ions through strong covalent BO_3^{3-} units [10]. In figure 1, the warwickite crystal is seen along the short axis, putting in evidence the ribbon-built structure. The two distinct metal sites are indicated. There are four distinct oxygen atoms: O1, which belongs in the Fe1–O–Fe2 path connecting two adjacent ribbons and is not bound to B, and O2, O3 and O4, which form the pseudo-trigonal BO_3 groups. In general, trivalent ions prefer the M(1) positions, which form the two inner columns of the ribbon; M(2) are preferentially occupied by the divalent ion as the outer octahedra have more crystallographic freedom to shelter larger ions [5].

As mentioned above, this occupation rule does not apply to the homometallic Fe warwickite, although it is strictly followed by the homometallic mixed valence Mn warwickite [6], of similar structure. From neutron diffraction [11] and Mössbauer spectroscopy [2–4] data it has been found that below 270 K there are two distinct Fe^{2+} and two distinct Fe^{3+} sites, equally populated; between 270 and 400 K, +2, +3 and +2.5 charge states are identified and above 400 K only +2.5 could be distinguished. Thus, in the low temperature

range, di- and trivalent metal cations occupy the two metal sites in the same proportion while above 400 K rapid electron hopping takes place between Fe^{2+} and Fe^{3+}, consistently with the average charge of +2.5. In the broad range 270–400 K, the two situations, charge ordering and electron hopping, coexist.

A theoretical study of the electronic structure and magnetic properties of the monoclinic phase of Fe_2OBO_3 has been done by using the LSDA + U local spin density method [7]. An order parameter was proposed to describe charge ordering, defined as the difference between occupancies of the extra t_{2g} electron of Fe^{2+} in crystallographically equivalent sites. This difference amounts to about 0.8 whereas the calculated total 3d charge difference remains very small. This was attributed to screening. The arrangement of +2 and +3 cations among the two crystalline sites proposed by Attfield *et al* [1] was found to be the most stable among some other distributions analysed, as far as LSDA + U calculation is concerned. However, when the electrostatic long range Madelung potential was considered, other distributions were found to be more stable. It is pointed out by the authors that some interaction between electrons and lattice must be relevant in determining the distribution of Fe^{2+} in the *background* of Fe^{3+} cations. As for magnetic interactions, it was shown that in Fe_2OBO_3 interribbon interaction plays the major role in determining the ferrimagnetic arrangement, through a strong anti-ferromagnetic exchange parameter between Fe1–Fe2 pairs sharing a common O between two neighbour ribbons. It has been found that LSDA calculation, which does not take into account electron correlation, does not reproduce ordering in the Fe_2OBO_3 lattice.

Balaev *et al* [12] have recently synthesized single crystals of the vanadium substituted warwickite $Fe_{1.91}V_{0.09}OBO_3$ and found evidence that the material crystallizes in the *Pnam* orthorhombic structure, with cell parameters very close to those of Fe_2OBO_3. No structural transition was found down to probably 4.2 K. The V-substituted warwickite also presents a 3D ferrimagnetic order but at a lower transition temperature (130 K). Mössbauer spectroscopy reveals the presence of three oxidation states of Fe, +2, +2.5 and +3, at room temperature. The charge state $Fe^{2.5+}$ has also been interpreted as indicative of rapid electron hopping. The presence of V^{2+} in site 2 reduces the occupancy of Fe^{2+} and Fe^{3+} at the edges of the ribbon. Nevertheless, both crystal sites remain almost equally occupied by the three oxidation Fe states. In contrast with the pure monometallic compound, no temperature range has been reported for the V-substituted material in which complete charge ordering occurs. These results reinforce the idea that the structural transition in Fe_2OBO_3 is closely related to charge ordering.

The indication that electron–lattice interaction is important in determining the charge distribution in Fe_2OBO_3 raises the question of the relationship between the electronic structure and geometry of the different phases of the compound. In addition, the fact that the substituted V warwickite does not present charge localization or structural transition makes this material an excellent example to be compared with the unsubstituted warwickite. In this paper we analyse the electronic structure of two crystalline phases of Fe_2OBO_3, namely the monoclinic ($T = 3$ K) and the orthorhombic ($T = 337$ K) phases [2], and of the V substituted warwickite, aiming at a better understanding of the relationship between electronic and crystal structures. We use the extended Hückel (eHT) method [13] in the high spin band (hsb) filling scheme, which has been considered in the study of another high spin oxy-borate, the mono-metallic Fe ludwigite [14]. The hsb scheme takes into account electron correlation in a semi-quantitative basis and allows a convenient extended Hückel description of the system.

2. Theory

Extended Hückel is a widely known semi-empirical tight binding method and its foundations concerning the calculation of electronic structure of molecules and solids can be found

elsewhere [13, 15]. Here, we point out some aspects of the theoretical approach which directly concern our study. The Hamiltonian matrix is given by the atomic orbital terms, H_{ii}, obtained from experimental ionization potentials, and off-diagonal terms H_{ij}, defined as $k(H_{ii}+H_{jj})S_{ij}$, where k is a conveniently chosen constant and S_{ij} the overlap integral between atomic orbitals i and j. In the present paper, we use standard empirical parameters[1] defined as follows. For O, $H_{2s,2s} = -32.3$ eV with $\zeta_{2s} = 2.275$, $H_{2p,2p} = -14.8$ eV with $\zeta_{2p} = 2.275$; for Fe, $H_{4s,4s} = -9.10$ eV with $\zeta_{4s} = 1.9$, $H_{4p,4p} = -5.32$ eV with $\zeta_{4p} = 1.9$, $H_{3d,3d} = -12.6$ eV with $\zeta_1 = 5.35$ and $\zeta_2 = 2.00$ in a linear double zeta combination with coefficients $c_1 = 0.5505$ and $c_2 = 0.6260$, respectively; for B, $H_{2s,2s} = -15.2$ eV with $\zeta_{2s} = 1.3$, $H_{2p,2p} = -8.5$ eV with $\zeta_{2p} = 1.3$.

A useful quantity is the so called crystal orbital overlap population (COOP), to investigate atom or orbital-pair interactions [15]; the integration of appropriately chosen COOP curves, throughout the occupied states (total COOP), gives quantitative estimates of bond orders. To obtain density of states (DOS) and COOP curves, a mesh of 192 reciprocal lattice k points was considered well suited for the 3D system; for the 1D ribbons we have used a set of 150 k points. As usual within the extended Hückel approach the Fermi level is defined as the highest occupied crystal orbital. Mulliken atomic charges are given by the integration of projected DOS curves.

The high spin band (hsb) filling scheme is based on experimental evidence that the metal cations are in high spin states [14]. In the present case, $S = 2$ for Fe^{2+} and $S = 5/2$ for Fe^{3+} [2, 3, 8]. It therefore relies on the localized character of spin distribution. The hsb filling scheme presents strict analogies with the semi-empirical treatment of spin interactions of Whangbo and co-workers [18]. In the case of the Fe warwickite, as for the Fe ludwigite [14], the picture is that of spin down extra electrons of Fe^{2+} moving in a frozen background of Fe^{3+} cations [19]. The scheme should be considered suitable if metal bands have nearly the same width and structure as those of molecular orbitals of isolated sub-units surrounding the metal. It is considered inadequate when bands coming from other parts of the system spread out in the same energy region as that of the high spin metal.

3. Crystal structure

In this section, we present some geometrical data, taken directly from the crystal structures of Fe_2OBO_3 obtained by Attfield *et al* [2], which will be useful to the theoretical analysis. In table 1, several next-neighbour distances are given for cation–oxygen and metal–metal pairs. The size of a given FeO_6 octahedron is estimated through the average Fe–O distance (r_{av}) and its degree of distortion is given by Δ. The latter has been obtained from the average of the square of the differences between Fe–O distances and r_{av} divided by r_{av}, in a given octahedron [16]. By mutually comparing the several values of r_{av} and Δ it is noticed that in the less symmetric monoclinic structure there is more similarity in the geometry around metal sites 1 and 2 than in the orthorhombic phase. Indeed, for the monoclinic and orthorhombic structures, Fe2 distortion is 1.8 and 4.3 times that of Fe1, respectively; the ratio $r_{av,1}/r_{av,2}$, on the other hand, is 1.00 (1.02) in the monoclinic (orthorhombic) phase. Therefore, the two metal sites are less equivalent in the orthorhombic structure. It can also be noticed that the monoclinic distortion affects the trigonal BO_3 group by reducing d_{B-O4} and enlarging d_{B-O2} and d_{B-O3} with respect to the more symmetric orthorhombic structure. Fe1–Fe1 distances are considerably smaller than Fe1–Fe2 distances in both structures.

Empirical estimates taken from valence bond sums (vbs) [17] predict, for the monoclinic phase, atomic charges of 2.37/2.54 for Fe1 and 2.40/2.56 for Fe2, when empirical bond valence

[1] Tables of parameters for extended Hückel calculations, collected by Santiago Alvarez, Universitat de Barcelona, 1993.

Table 1. Some distances of Fe_2OBO_3 lattices (in Å).

Monoclinic structure (3 K)						
$a = 9.2503$ Å, $b = 9.3835$ Å, $c = 3.1688$ Å and $\beta = 90.220°$						
Cation–oxygen distances (short/long)						
	O1	O2	O3	O4	r_{av}	Δ
Fe1	1.986/2.013/2.074	2.134/2.224	2.082	—	2.085	0.0014
Fe2	1.919	2.048	2.002/2.227	2.159/2.139	2.082	0.0025
B	—	1.398	1.397	1.353	—	—
Fe–Fe distances						
	Intra-ribbon	Inter-ribbon	Along c (1–1)	Along c (2–2)	—	—
1–1	2.957/2.961	—	—	—	—	—
1–2	3.277/3.299	3.393/3.472	3.169	3.169	—	—
Orthorhombic structure (337 K)						
$a = 9.2495$ Å, $b = 9.3945$ Å, $c = 3.1779$ Å						
Cation–oxygen distances						
	O1	O2	O3	O4	r_{av}	Δ
Fe1	2.006/2.143/2.143	2.189/2.189	2.087	—	2.126	0.0009
Fe2	1.841	2.185	2.200/2.200	2.037/2.037	2.083	0.0039
B	—	1.349	1.342	1.486	—	—
Fe–Fe distances						
	Intra-ribbon	Inter-ribbon	Along c (1–1)	Along c (2–2)	—	—
1–1	2.990/2.990	—	—	—	—	—
1–2	3.253/3.253	3.413/3.527	3.178	3.178	—	—

parameters are related to $2+/3+$ oxidation state. For the orthorhombic structure, on the other hand, one gets $2.11/2.26$ for Fe1 and $2.49/2.67$, for Fe2, respectively. These values indicate propensity of site 1 in the orthorhombic structure to shelter Fe^{2+}, with atomic charge 2.11, while, for site 2, the empirical estimates are more consistent with the oxidation state Fe^{3+} (atomic charge 2.67). This is in contrast to the monoclinic phase, in which valence bond charges tend to stay in the vicinity of $+2.5$ for both sites.

The above geometry-based analysis points at the monoclinic phase being structurally more flexible than the orthorhombic one in determining site preferences of di- and trivalent cations in Fe_2OBO_3. Clearly, this feature might help other electronic mechanisms in establishing the charge localization state of the Fe warwickite, which is based on equal Fe^{2+} and Fe^{3+} distribution among sites.

4. Results

In order to understand the interplay between local and extended properties we investigate separate sub-units of Fe_2OBO_3, carved out from the crystal structure in both phases. Figures 2 and 3 show the calculated electronic structure of the two isolated and crystallographically distinct FeO_6 monomers, and of extended calculations for the 1D ribbon and 3D models for both the monoclinic (figure 2) and orthorhombic (figure 3) crystals. The 1D model consists

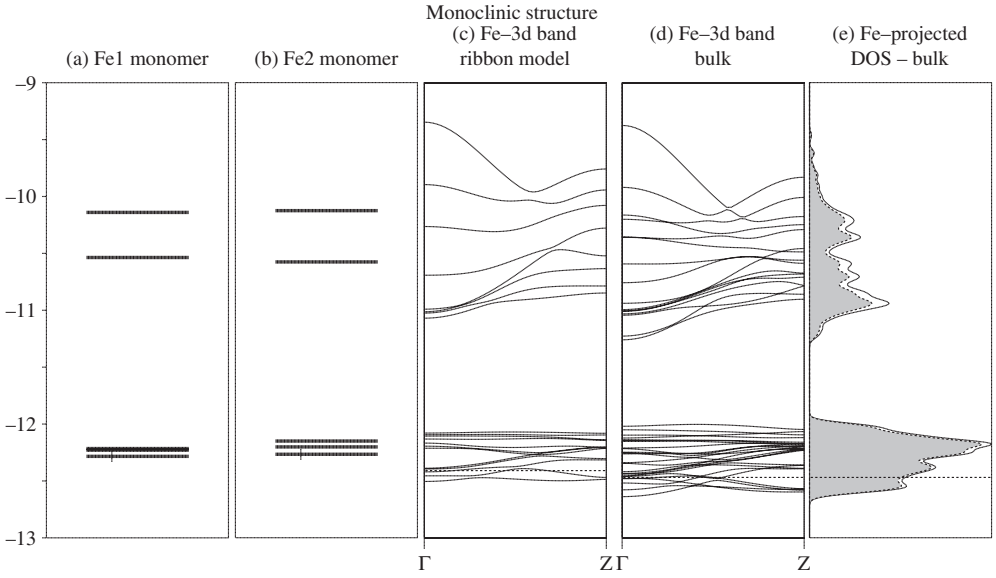

Figure 2. Electronic structure of several sub-units of the monoclinic phase of Fe_2OBO_3: (a), (b) molecular energy levels of FeO_6 monomers showing the occupancy of the extra electron in an Fe^{2+} oxidation state; (c), (d) the Fe 3d band structure of the 1D sub-unit and of the 3D crystal (bulk), respectively; (e) the Fe-projected DOS for the 3D crystal (dark area). Note the strong Fe 3d character of the total DOS curve. Energies are in eV. Occupancy and Fermi level correspond to the hsb filling scheme.

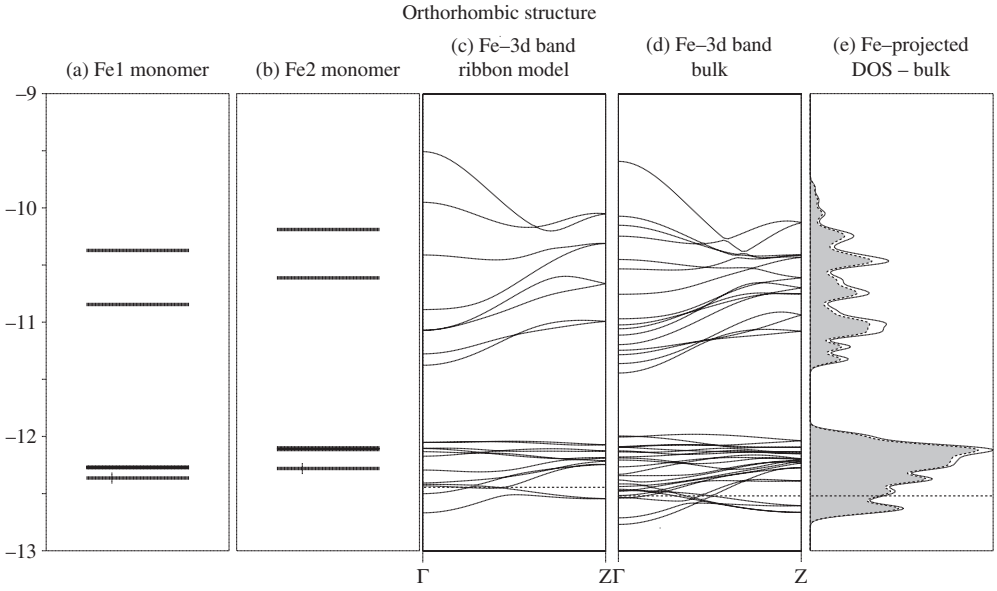

Figure 3. Electronic structure of several sub-units of the orthorhombic phase of Fe_2OBO_3: (a), (b) molecular energy levels of FeO_6 monomers showing the occupancy of the extra electron in an Fe^{2+} oxidation state; (c), (d) the Fe 3d band structure of the 1D sub-unit and of the 3D crystal (bulk), respectively; (e) the Fe-projected DOS for the 3D crystal. Note the strong Fe 3d character of the total DOS curve. Energies are in eV. Occupancy and Fermi level correspond to the hsb filling scheme.

of an isolated four octahedron wide ribbon, carved out directly from the crystal structure (see figure 1). DOS curves correspond to projections on the two metal sites.

The octahedral field splitting is clearly seen in all calculations, with three levels below −12 eV (coming from degeneracy breaking of the t_{2g} group) and two levels above −11.5 eV (e_g group). For the FeO_6 monomers, the cubic splitting is 1.68 eV/1.57 eV for monoclinic (figure 2) and 1.42 eV/1.49 eV for orthorhombic (figure 3) phases in site 1/2. The cubic separation is smaller in the extended models, as expected, due to dispersion. For the monoclinic phase (figure 2), one gets 1.01 eV/0.76 eV, respectively, for the 1D/3D model, and for the orthorhombic phase (figure 3) the splitting is 0.68 eV/0.54 eV for the 1D/3D model. The monoclinic values are in reasonable agreement with the 2 eV crystal splitting found by Leonov *et al* [7] and are slightly higher than that obtained for the orthorhombic structure. This is a consequence of bigger monomer sizes (Fe1) and distortions (Fe2) in the latter.

The strong similarity of the structure of the monomer molecular orbitals with that of the band levels of the extended systems, seen in figures 2 and 3, provides a quantitative argument for the use of the high spin band filling scheme. Note that the extended bands clearly preserve the cubic splitting character of the Fe 3d monomer levels, with comparable cubic gap and a closely related 3d energy range. It could also be noted that the Fe-projected density of states is by far the main contribution the to total DOS in the 3d band (figures 2(e) and 3(e)), indicating small O contributions. These results point towards a localized characted of Fe bands in Fe_2OBO_3, an important feature to justify the use of the high spin band (hsb) filling scheme.

Within hsb, the molecular levels are filled according to the metal spin state, thus defining a high spin configuration in the one electron approach. For $S = 5/2$ (Fe^{3+}), the five, say, spin up electrons are arranged according to Hund's rule, filling the five typically Fe 3d levels of the monomer. For $S = 2$ (Fe^{2+}), there are four singly occupied molecular levels plus double occupancy in the lower t_{2g} level. For comparison, in figures 2 and 3 (see panels (a) and (b)), we have indicated the molecular level which would be occupied with the sixth (spin down) electron if each of the isolated monomers held a Fe^{2+} cation.

The molecular orbital (MO) analysis of the isolated monomers is entirely consistent with geometrical parameters (see table 1) and vbs estimates for the different sites, confirming, within the MO point of view, that the electronic equivalence of metal sites is more noticeable in the monoclinic phase. Note, for instance, the energy separation of the lowest level in each case. From the monomer results (figures 2 and 3), site 1 can be noted to be more stable in both structures but the energy difference between the lowest t_{2g} of both sites is, however, negligible in the monoclinic (0.01 eV), being one order of magnitude larger (0.08 eV) in the orthorhombic case, therefore indicating less tendency for site preference in the low temperature phase.

In order to determine band occupancy within the hsb filling scheme, one follows the rule established above, consistently with the high spin state of the metal cations. In the 1D model one has four Fe atoms per unit cell; therefore, $4 \times 5 = 20$ spin up electrons associated with the Fe^{3+} background fill, with single occupancy, the 20 3d bands. The two extra electrons per unit cell provide spin pairing at the two lowest bands of the t_{2g} group (below −12 eV). If one defines a spin down Fermi level, it comes to be located inside the t_{2g} band at −12.41 eV/−12.44 eV for monoclinic/orthorhombic phases (figures 2(c) and 3(c)). In the 3D model calculation, one benefits from the same reasoning, thus four extra Fe^{2+} electrons per unit cell provide spin pairing at the four lowest t_{2g} bands, with the Fermi energy at −12.47 eV/−12.52 eV for monoclinic/orthorhombic crystal phases (figures 2(d) and 3(d)). The system is described as metallic. Leonov *et al* [7] have found a gap of ∼0.3 eV to be associated with electron correlation. Therefore, in the present one-electron calculation no gap is to be expected.

In an extended Hückel study of the mixed-valent ludwigite $Fe_3O_2BO_3$, an hsb gap was found, of ∼0.2 eV [14], related to small lattice distortions. The electronic gap in these two

Table 2. Calculated atomic charges.

	Fe1	Fe2	B	O1	O2	O3	O4
1D model							
Monoclinic	0.86	1.60	—	−1.49	−1.51	−1.49	−1.49
Orthorhombic	0.93	1.60	—	−1.50	−1.53	−1.50	−1.50
3D model							
Monoclinic	1.00	1.51	1.47	−1.00	−1.01	−0.99	−0.98
Orthorhombic	1.08	1.53	1.47	−1.03	−1.01	−0.96	−1.08

mixed-valent Fe oxy-borates has, therefore, a different origin. It is worth noticing that, while small changes in the gap of Fe_2OBO_3 are associated with the structural transition, in the ludwigite, the octahedral distortions responsible for the appearance of the electronic gap are not directly related to the structural transition observed for the compound [14, 20].

Table 2 shows the calculated atomic charges for the 1D sub-unit and the 3D lattice in both structures. It can be noticed that the difference between Fe1 and Fe2 charges is slightly bigger in the 1D model, being 0.74/0.67 for the monoclinic/orthorhombic phase. Bulk (3D model) calculation gives a difference of 0.51 and 0.55, respectively, for the monoclinic and orthorhombic crystalline structure. The bigger site separation of the ribbon model indicates stronger localization. This suggests that inter-ribbon interaction could provide paths for charge transfer between sites, in qualitative agreement with the LSDA$+U$ calculation of spin coupling constants [7]. These authors have found inter-ribbon about twice as big as intra-ribbon coupling constants. The role of inter-ribbon interactions will be dealt with in the next section.

4.1. Fe–Fe dimers

In this section we investigate the electronic structure of different Fe–Fe dimers in the material, these consisting of isolated molecular fragments Fe_2O_{10}, for edge-sharing, and Fe_2O_{11}, for vertex-sharing oxygen octahedra. The analysis is intended to examine local effects on metal–metal interactions, which are not clearly seen in extended calculations. We consider the metal pairs whose Fe–Fe distances are shown in table 1. In the orthorhombic structure, there are six distinct dimers, corresponding to the five shortest metal–metal distances, due to the fact that there are two pairs, 1–1 and 2–2, piling along the *c*-axis, with the same inter-atomic distance. In the monoclinic structure, symmetry lowering introduces two more dimers. There are thus eight sub-units to be investigated in this case.

In figure 4, six Fe–Fe monoclinic pairs are illustrated, namely four intra-ribbon (figure 4(a)) and two inter-ribbon pairs (figure 4(b)). Two more exist (not shown), connecting 1–1 and 2–2 pairs along the *c*-axis, in the chains denoted 1 and 2 in figure 4(a). There are then six intra-ribbon pairs in the monoclinic case. For the orthorhombic structure, the intra-ribbon pairs denoted *long* and *short* (figure 4(a)) colapse into two single 1–1 and 1–2 Fe pairs, due to the ribbon stretching up in the transition to the orthorhombic phase.

Our interest concerns the effect of the structural transition on Fe–Fe bonds mediated by the ligands. As charge ordering in Fe_2OBO_3 is associated with spin density distribution of the extra electron of Fe^{2+}, the analysis is focused on the t_{2g} group. In fact, actual calculations on different dimers have shown a well characterized t_{2g}–e_g separation, with a gap of 1.0–1.5 eV, between the six lowest (t_{2g}) and the four highest (e_g) MO levels of the metal dimer.

Within molecular orbital theory, stronger interaction is related to larger electron population in the overlap region of the dimer. If one is interested in the effects of the lattice geometry

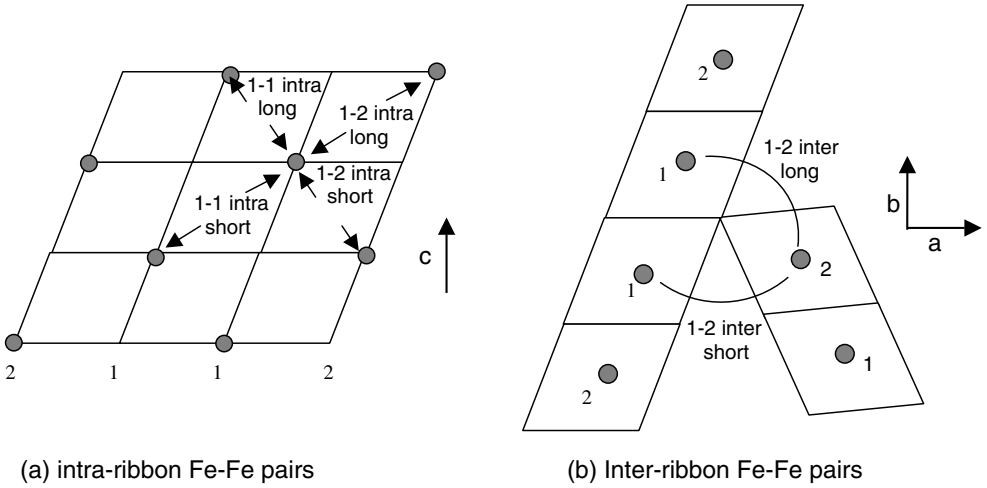

Figure 4. Schematic view of six distinct Fe–Fe pairs of the monoclinic structure. (a) Intra-ribbon pairs; 1–1 and 2–2 pairs along c (no arrows shown) connect next neighbours in columns 1 and 2 respectively. (b) Inter-ribbon pairs.

Table 3. Fe–Fe dimer interaction energies in eV.

	Intra-ribbon pairs						Inter-ribbon pairs	
	1–1 short	1–1 long	1–2 short	1–2 long	1–1 (c)	2–2 (c)	1–2 short	1–2 long
Monoclinic	0.204	0.151	0.053	0.062	0.216	0.220	0.093	0.131
Orthorhombic	0.225		0.125		0.291	0.217	0.172	0.185

in the dynamics of electronic charge distribution, one could interpret the overlap electronic densities as paths for charge transfer. This simple picture provides an atomistic-geometrical description of the compound and allows a comparison between lattice based processes of charge distribution in the two different crystal phases of the warwickite. With regard to charge localization in Fe_2OBO_3, one is mainly concerned with charge transfer between different sites, since the charge ordered state has an equal distribution of Fe^{2+} and Fe^{3+} in both sites. A consistent picture would be that of a sea of extra Fe^{2+} electrons jumping from site to site, the jumping energy competing with electron repulsion and electrostatic long range interaction.

To estimate the interaction energy of two monomers we have calculated the difference ΔE between the total t_{2g} energy of the dimer and that of the separated monomers [21]. The calculated values for ΔE are shown in table 3 for the several pairs. Note that in the monoclinic phase the interaction energy of 1–2 dimers turns out to be about 50% smaller than the value obtained for the orthorhombic phase, indicating less overlap density in the former. These results suggest that in the higher temperature (orthorhombic) crystalline structure of Fe_2OBO_3 local geometry is more favourable for hopping between sites, in agreement with experimental data on Mössbauer spectroscopy [1, 3]. As temperature lowers, the hopping energy decreases as a result of monoclinic local distortions, which in this way tends to localize the electronic distribution around the distortion, favouring local ordering. Thus, electron–lattice interaction during the structural transition would help charge ordering by stabilizing preferred distributions possibly set in through other more complex electronic mechanisms, such as electrostatic and magnetic interactions [1, 7].

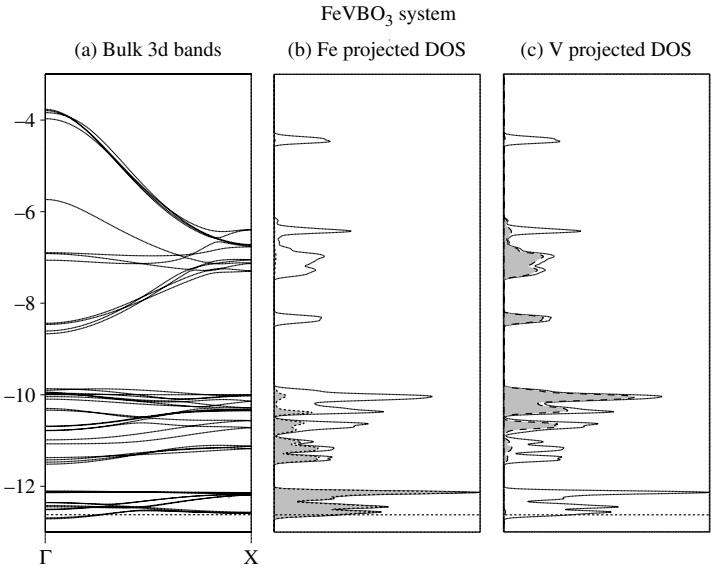

Figure 5. The electronic structure of a perfect stoichiometry $FeVOBO_3$ system. (a) Band structure; (b) and (c) Fe and V projected DOS. Dotted line: Fermi level. Energies are in eV.

The dimer description of actual interactions which take place in the crystalline environment can be justified by the localized nature of the spin distribution which, as shown above, is reasonably reproduced by the extended band structure description of the material. The analysis aims at providing basic understanding of local geometrical effects, thus, concerning actual quantitative results, the isolated sub-unit results must be taken with care.

4.2. The vanadium–iron warwickite

If electron–lattice interaction is physically related to the orthorhombic–monoclinic transition of Fe_2OBO_3, as discussed in the previous section, inter-ribbon interaction would be expected to play a role in the structural change since the latter occurs while charge ordering, a process which involves charge transfer between sites 1 and 2, sets in. In $Fe_{1.91}V_{0.09}OBO_3$, no structural transition or charge ordering was found, in spite of its similarity with the pure Fe warwickite [12]. Understanding the effect of V substitution could then bring new insight into the properties of the warwickite. This is examined in the present section.

$Fe_{1.91}V_{0.09}OBO_3$ crystallizes in the orthorhombic structure, with lattice parameters very close to those of Fe_2OBO_3 ($a = 9.2317$ Å, $b = 9.3831$ Å, $c = 3.1727$ Å) [12]. Since the detailed structural data were not provided, we have used in the calculations the orthorhombic structure of the unsubstituted compound.

Requirement of translational symmetry leads one to consider different stoichiometries as models for the disordered $Fe_{1.91}V_{0.09}OBO_3$ system. We assume that V occupies crystal site 2 with oxidation state +2, according to experimental evidence [12]. Figure 5 shows the results of calculations performed on an $FeVOBO_3$ perfect stoichiometry model system. Cubic splittings of Fe 3d and V 3d orbitals are clearly seen, with the superposition of $Fe(e_g)$ and $V(t_{2g})$ in the energy range of -11.5 to -10 eV. Metal projected DOS (figure 5(b)) reveals an almost independent $Fe(t_{2g})$ band below -12 eV, with very small V contribution at the Fermi level. Boron bands spread from -7 to -4 eV.

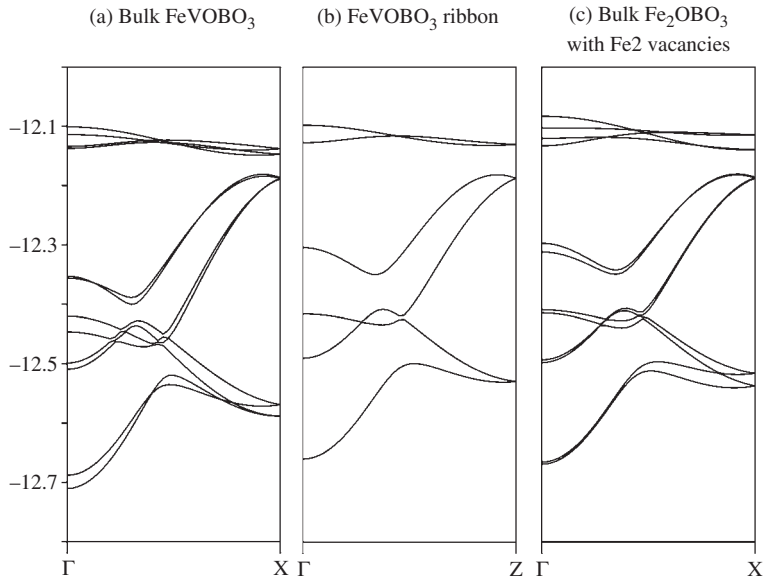

Figure 6. The lower t_{2g} band structure of (a) 3D and (b) 1D models of the substituted warwickite and (c) of a prototype Fe_2OBO_3 system. Note the similarity between the three band structures. Energies are in eV.

Within the hsb scheme one thinks of $(4 \times 5) + (4 \times 3) = 32$ majority spin electrons per unit cell, coming from the four $Fe(3d^5)$ and four $V(3d^3)$ cations, respectively. These fill in the $(4 \times 5) + (4 \times 3) = 32$ crystal levels corresponding to the t_{2g} and e_g groups of Fe plus the t_{2g} group of V. In this way, the highest occupied crystalline level stays at the top of the $V(e_g)$ band and has energy approximately -10 eV at point Γ (see figure 5). The system constitutes an electronically stable, insulating prototype material with a gap of about 1.5 eV. If some V^{2+} cations of the perfect stoichiometry system are substituted by divalent Fe, the extra electrons of Fe^{2+} occupy the half filled lowest Fe t_{2g} band, thus defining the (minority spin) Fermi level (shown in figure 5). This almost perfect stoichiometry system behaves as a conductor. With increasing Fe^{2+} content, the Fermi level will stay in the lower t_{2g} bands, with no qualitative changes as for the relative position respectively with the 3d bands. From these results, the basic electronic structure of the substituted warwickite could be expected to be very similar to that of the unsubstituted compound. This is in agreement with experimental data, which found no essentially different conductivity and magnetic behaviour of $Fe_{1.91}V_{0.09}OBO_3$ as compared to that of Fe_2OBO_3 [12]. Note that in the present analysis it was assumed that V^{2+} cations are in a high spin state. The justification of the validity of the Hund's rule could be ascribed to the narrow width of the V t_{2g} band (see figure 5). Also, in another bimetallic warwickite, vanadium was found to be magnetic [22].

To investigate the role of vanadium in the interactions near the Fermi level, we consider in more detail the t_{2g} band of the $FeVOBO_3$ system, assuming that a small amount of V^{2+} is substituted by Fe^{2+}. In figure 6, the bulk (3D) band structure is compared with that of the 1D ribbon. It can be noticed that bulk bands are very nearly simple superpositions of two 1D bands, similarly to what was observed in $MgTiOBO_3$ [10]. By contrast, in none of the two crystal phases of the unsubstituted Fe_2OBO_3 compound is this superposition effect observed (see figures 2 and 3).

This suggests that the presence of vanadium hinders inter-ribbon interaction, since band superposition indicates lack of crystal orbital interactions. The argument could be further justified if one examines the band structure of a hypothetical Fe_2OBO_3 warwickite in which Fe atoms in site 2 have been removed (figure 6(c)). The artificially created Fe vacancies at the borders of the ribbon aim at eliminating inter-ribbon interaction (see figure 4). The striking similarity between figures 6(a) (bulk $FeVOBO_3$ system) and (c) (bulk Fe_2OBO_3 + vacancies) suggests that, within the overall view of band structure, V acts as a vacancy as far as inter-ribbon interactions near the Fermi level are concerned. It could be pointed out that in both Fe–V and Mg–Ti warwickites, where the effect was observed, the divalent metal (V and Mg) has lower electronegativity than the trivalent transition metal, pushing up the divalent d bands. This causes energy separation between di- and trivalent metal bands. If the Fermi level is located at the lower trivalent t_{2g} bands where inter-ribbon connection paths get lost, the hindrance effect may be manifested. This is the case with the two bimetallic warwickites.

A quantitative estimate of inter-ribbon interactions could be made by comparing Fe–Fe with Fe–V inter-ribbon COOPs at the Fermi level. The quantity gives the contribution of the atom pair to bond order. For *long* inter-ribbon distances (see figure 4) one gets −0.016 for Fe1–Fe2 and −0.004 for Fe1–V2. Inter-ribbon *short* pairs give 0.011 and 0.004 for Fe1–Fe2 and Fe1–V2, respectively. These results are consistent with the behaviour of t_{2g} bands, by showing smaller inter-ribbon COOP in the V substituted system.

Additional calculations were done by varying the content of V in the unit cell in order to simulate the effect of small V concentrations. As expected, one finds that the hindrance effect in the band structure reduces as the V content decreases, a correct trend towards the results found in the unsubstituted warwickite.

The above results indicate that the presence of vanadium in site 2 causes a decrease in inter-ribbon Fe–Fe interactions, with a consequent reduction of charge transfer paths. This could be an important mechanism to explain the stability of the orthorhombic phase in the substituted warwickite. It is reasonable to expect that small V amounts could act so as to make it difficult for local monoclinic distortions to percolate in the Fe_2OBO_3 lattice, since these distortions are known to be associated with charge localization processes.

The calculated atomic charges of the substituted compound turn out to be very different when two band filling schemes are used. Within the usual (*aufbau*) scheme, one gets, respectively, −0.787 and 3.133 for Fe and V, an unrealistic result. By contrast, the hsb filling procedure leads to the values 1.912 and 0.602, respectively, for atomic charges of Fe and V, consistently with the oxidation states +3 and +2 of the metal cations. As Fe bands stay below V bands, calculation of Mulliken charges in the (diamagnetic) ground state leads to electron excess in Fe orbitals. By allowing electrons to occupy the higher 3d metal states of vanadium, the hsb approximation reverses this tendency. This qualitative improvement could be considered an excellent result of the high spin band procedure in describing the bimetallic material.

Even though some differences might occur in the calculated quantities for the substituted warwickite, if the actual crystal structure was used, we believe that our main conclusions would not be significantly altered, due to the general aspect of the analysis and to the fact that the two compounds have essentially the same crystalline structure.

5. Conclusion

A detailed theoretical study was done on the electronic structure of the pure Fe_2OBO_3 and substituted $Fe_{1.91}V_{0.09}OBO_3$ warwickites, by using the extended Hückel method within the

high spin band filling scheme. The orthorhombic and monoclinic phases of Fe_2OBO_3 were considered and calculations were performed on bulk and on different molecular and extended sub-units carved out directly from the crystal structure.

Calculations have shown that the two crystal phases of Fe_2OBO_3 present differences as concerns electron–lattice interactions. For instance, it has been found that inter-site Fe1–Fe2 interactions mediated by oxygen are ∼50% smaller in the monoclinic structure. Since in the Fe warwickite structural transition is associated with charge distribution, lowering of inter-site interactions, which in turn reduces charge transfer, was suggested to stabilize local monoclinic distortions which might set in through other mechanisms, such as electrostatic long range interactions as suggested by Attfield *et al* [1, 2]. This local stabilization could allow distortions to percolate in the lattice.

Another significant geometry effect of the structural transition is related to the two crystallographically distinct FeO_6 monomers. In the monoclinic phase, $Fe1O_6$ and $Fe2O_6$ oxygen octahedra were found to be quasi-equivalent, with the relevant site energy difference being 0.01 eV. In the orthorhombic structure the same quantity is about one order of magnitude larger. As a result, below 317 K, the ability of different sites to hold the divalent metal becomes comparable, creating conditions for different charge distribution arrangements in the monoclinic phase to occur. This basic electron–lattice mechanism could help understanding the broad temperature range of the charge ordering transition in Fe_2OBO_3.

In the vanadium substituted warwickite, calculations have shown that the presence of V hinders inter-ribbon interaction at the Fermi level, lowering, with regard to the orthorhombic structure of the unsubstituted compound, inter-site charge transfer between ribbons. As a consequence, some transport paths of the extra electron of Fe^{2+}, due to small amounts of vanadium, would be lost, making it difficult for monoclinic distortions to percolate in the lattice. This would explain why $Fe_{1.91}V_{0.09}OBO_3$ does not undergo a structural transition. These results corroborate the idea that inter-ribbon paths are the key feature to understand structural transition and charge ordering in Fe_2OBO_3.

Fe–Fe interactions inside a sub-lattice were found to be stronger than those connecting different Fe sub-lattices and nearly the same in both orthorhombic and monoclinic structures. These bonds provide paths for conductivity without modifying a given charge distribution. This result could explain the similarity in the conductivity regimes in both phases [1, 2]. The slight difference in the activation energy found between the two crystal structures could be associated with the differences in Fe–Fe bonds between sites 1 and 2, discussed above.

The hsb calculated metal charges are in agreement with the oxidation states of the metals in both materials. In particular, a striking improvement was obtained in the V substituted compound, for which the usual ground state band filling procedure leads to an unrealistic excess of electrons in Fe. This was considered an excellent result of the hsb-eHT approach in the description of the bimetallic warwickite, where different electronegativities tend to over-populate one of the metal orbitals if the usual *aufbau* filling scheme is used.

In spite of the simplicity of the one electron approach, new insight has been provided in the present study as to the role of electron–lattice interactions in the pure and substituted warwickites. It is expected that this analysis could help future experimental and theoretical studies in these and similar compounds.

Acknowledgment

All calculations in this paper were done with the *yaehmop* package, developed by Dr Greg Lundrum.

References

[1] Attfield J P, Bell A M T, Rodrigues-Martinez L M, Greneche J M, Cernik R J, Clarke J F and Perkins D A 1998 *Nature* **396** 655–8

[2] Attfield J P, Bell A M T, Rodrigues-Martinez L M, Greneche J M, Retoux R, Leblanc M, Cernik R J, Clarke J F and Perkins D A 1999 *J. Mater. Chem.* **9** 205–9

[3] Douvalis A P, Papaefthymiou V, Moukarita A, Bakas T and Kallias G 2000 *J. Phys.: Condens. Matter* **12** 177–88

[4] Douvalis A P, Papaefthymiou V, Moukarita A and Bakas T 2000 *Hyperfine Interact.* **126** 319–27

[5] Norrestam R, Kritikos M and Sjödin A 1995 *J. Solid State Chem.* **114** 311–6

[6] Goff R J, Williams A J and Paul Attfield J 2004 *Phys. Rev.* **70** 014426(1-5)

[7] Leonov I, Yaresco A N, Antonov V N, Attfield J P and Anisimov V I 2005 *Phys. Rev.* B **72** 014407(1-7)

[8] Continentino M A, Pedreira A M, Guimarães R B, Mir M, Fernandes J C, Freitas R S and Ghivelder L 2001 *Phys. Rev.* **64** 014406(1-6)

[9] Takéuchi Y, Watanabe T and Ito T 1950 *Acta Crystallogr.* **3** 98–107

[10] Matos M, Hoffmann R, Latgé A and Anda E V 1996 *Chem. Mater.* **8** 2324–30

[11] Attfield J P, Clarke J F and Perkins D A 1992 *Physica* B **180/181** 581–4

[12] Balaev A D, Bayukov O A, Vasilév A D, Velikanov D A, Ivanova N B, Kazak N V, Ovchinnikov S G, Abd-Elmeguid M and Rudenko V V 2003 *J. Exp. Theor. Phys. (JETP)* **97** 989–95
Kazak N V, Balaev A D, Ivanova N B and Ovchinnikov S G 2005 *Physica* B **359–361** 1324–6

[13] Hoffmann R 1963 *J. Chem. Phys.* **39** 1397–412
Whangbo M-H and Hoffmann R 1978 *J. Am. Chem. Soc.* **100** 6093–8

[14] Matos M 2004 *J. Solid. Stat. Chem.* **177** 4605–15

[15] Hoffmann R 1988 *Solids and Surfaces* (New York: VCH)

[16] Shannon R D 1976 *Acta Crystallogr.* A **32** 751

[17] Brown I D and Altermatt D 1985 *Acta Crystallogr.* **41** 244–7
Brese N E and O'Keeffe M 1991 *Acta Crystallogr.* B **4** 192–7

[18] Whangbo M-H, Dai D and Koo H 2005 *Solid State Sci.* **7** 827–52

[19] Latgé A and Continentino M A 2002 *Phys. Rev.* **66** 094113(1-5)

[20] Mir M, Guimarães R B, Fernandes J C, Continentino M A, Dorigueto A C, Mascarenhas Y P, Ellena J, Castellano E E, Freitas R S and Ghivelder L 2001 *Phys. Rev. Lett.* **87** 147201

[21] Hoffmann R 1971 *Acc. Chem. Res.* **4** 1–9

[22] Continentino M A, Fernandes J C, Guimarães R B, Boechat B, Borges H A, Valarelli J V, Haanappel E, Lacerda A and Silva P R J 1996 *Phil. Mag.* **73** 601